



Diesel soot oxidation over silver-loaded SiO₂ catalysts

Grisel Corro^{a,*}, Umapada Pal^{b,1}, Edgar Ayala^a, Esmeralda Vidal^a

^a Instituto de Ciencias, Benemerita Universidad Autonoma de Puebla, 4 Sur 104, 72000 Puebla, Mexico

^b Instituto de Física, Benemerita Universidad Autonoma de Puebla, Apdo. Postal J-48, 72570 Puebla, Mexico

ARTICLE INFO

Article history:

Received 21 March 2012
Received in revised form
19 September 2012
Accepted 3 October 2012
Available online 12 November 2012

Keywords:

Diesel soot
Soot oxidation
Ag/SiO₂ catalyst
Emissions abatement

ABSTRACT

The catalytic behavior of Ag-loaded fumed SiO₂ has been investigated for diesel soot oxidation. The diesel soot generated by burning pure Mexican diesel in laboratory was oxidized under air flow in presence of the catalyst inside a tubular quartz reactor in between 25 and 600 °C. UV–vis optical spectroscopy was utilized to study the electronic state of silver in Ag/SiO₂ catalysts. The soot oxidation was seen to be strongly enhanced by the presence of metallic silver on the catalyst surface, probably due to the formation of superoxide ion O₂⁻. During the catalytic process, the Ag₂O species on the catalyst acts as a strong oxidizing agent which gets reduced readily by the soot carbon to metallic Ag. The Ag/SiO₂ catalysts exhibited strong performance for diesel soot oxidation below 300 °C. Mechanical mixing of extra SiO₂ with 3% Ag loaded SiO₂ resulted a further increase of soot oxidation rate, probably due to the increased interactions of O₂⁻ and soot particles through the highly porous surface of SiO₂.

© 2012 Elsevier B.V. All rights reserved.

1. Introduction

The most effective and widely applied after-treatment technology for the control of particulate matter (PM) is based on diesel particulate filter (DPF) [1–3]. These devices perform the filtration of exhaust gases by removing a significant fraction of PM, which adheres to the filter walls, needing a periodic regeneration of DPF to remove the entrapped soot to avoid increased pressure drop at the exhaust.

The regeneration process can be carried out by the injection of extra fuel during the combustion of PM. However, this implies an extra fuel consumption and reduction of engine efficiency. Moreover, excessive heating caused by extra fuel consumption can damage the filter and other after treatment devices. Thus, several efforts have been made to find alternative solutions for filter regeneration at lower temperature. In one approach, an oxidation catalyst is deposited on the filter which allows its regeneration in a continuous or periodic manner during the regular operation of the system [4]. The catalyst accelerates the oxidation of diesel PM at the exhaust temperatures (typically in the 300–400 °C range) during the regular operation of the engine. In absence of the catalyst, particulates can be oxidized at appreciable rates only in the temperature range of 550–650 °C, which can occur only at full load conditions. However, the catalytic approach also has several

drawbacks: catalytic filter regeneration is very complex because of the complexity of reaction conditions. Moreover, the process is very slow because of the poor soot/catalyst contact. Another operative problem arises from the wide variation of temperature (200–600 °C) of the exhaust gases, depending upon the engine load. Thus, the selection of the catalyst is trivial as it should have high thermal stability and operate efficiently at lower temperatures.

For the above purpose, a wide variety of catalytic materials of distinct characteristics has been studied, targeting to increase the contact area between the soot particle and the catalyst, like fuel borne catalyst additives or molten salts catalysts, which can wet the soot surface and therefore decrease the oxidation temperature [5–7]. The use of NO₂ as oxidant has also been observed to decrease the soot combustion temperature [8–10].

Silver is known to be an efficient partial oxidation catalyst which has been used industrially for epoxidation of ethylene [11,12] and oxi-dehydrogenation of methanol to formaldehyde [13–15]. Other applications in which silver has shown high performances are the NO_x abatement [16,17], and oxidation of methane, carbon monoxide and organic volatile compounds [18–20]. Ag deposited over CeO₂ has higher carbon gasification efficiency in comparison with other noble metals [21,22]. The potentiality of silver deposited on Al₂O₃ for the carbon particle oxidation in the presence of NO_x and oxygen has been demonstrated recently [23]. Silver-based catalysts appear to be the most promising but are relatively inactive at temperatures below 350 °C [24].

As the fumed SiO₂ presents a very high surface area (550 m² g⁻¹), it can increase the residence time and deposition rate of carbon particles over the catalyst surface, thereby increasing the probability of interaction between the carbon particles and the

* Corresponding author. Tel.: +52 222 2295500x7294.

E-mail addresses: griselda.corro@correo.buap.mx (G. Corro), upal@sirio.ifuap.buap.mx (U. Pal).

¹ Tel.: +52 222 2295610.

active sites of the catalyst, and with the active oxygen species produced on Ag surface. Therefore, a catalyst consisting Ag and fumed silica (Ag/SiO_2) is expected to present high oxidation activity at temperatures below 300°C . The above mentioned characteristics of silver and fumed SiO_2 lead us to investigate the behavior of Ag/SiO_2 catalyst on the oxidation of diesel soot particles.

UV–vis absorption spectroscopy is a useful technique for studying electronic properties of heterogeneous catalysts [25–29]. The technique can be used to detect the atomic, ionic, and cluster states of silver, which exhibit characteristic absorption bands in UV–vis spectral range [30], present in a solution or in a supported catalyst [31]. While Ag^+ ions reveal their characteristic absorption bands in the 190–230 nm spectral range, silver atoms (Ag^0) reveal their characteristic bands in between 250 and 330 nm. On the other hand, small Ag_n clusters generally reveal their characteristic absorption bands in the 330–360 nm and 440–540 nm spectral ranges. Light absorption by large silver clusters (>10 nm), crystallites or aggregates manifest pronounced resonance bands in between 400 and 500 nm due to collective oscillation of their conduction electrons, known as surface plasmon resonances (SPRs), with features providing the information about their size, shape, and, interactions with the surrounding ambient [30,32–39].

In this study we have investigated the role of electronic state of silver in Ag/SiO_2 catalyst on the oxidation of diesel soot particles. Diffuse reflectance spectroscopy (DRS), has been utilized to determine the oxidation state of the catalyst. Ag-loaded fumed SiO_2 has been demonstrated as a stable, effective catalyst for diesel soot oxidation. The catalytic behavior of Ag/SiO_2 has been correlated to the electronic state of the loaded silver.

2. Experimental

2.1. Catalysts preparation

The fumed SiO_2 supplied by Aldrich (99.9%) was used as a support material for the preparation of Ag/SiO_2 catalyst. The catalyst was prepared by impregnation using an aqueous solution of silver nitrate (3 wt%). After impregnation, the catalyst was dried at 50°C overnight, and then calcined in air for 6 h at 450°C , after which it is called as calcined 3% Ag/SiO_2 . A reference SiO_2 support was prepared in the same way using only distilled water, this support is called as calcined SiO_2 . A part of the calcined 3% Ag/SiO_2 catalyst was reduced in pure hydrogen flow for 4 h at 500°C , and named as reduced 3% Ag/SiO_2 .

2.2. Catalysts characterization

The elemental composition of the calcined 3% Ag/SiO_2 and reduced 3% Ag/SiO_2 catalysts was analyzed using energy dispersive X-ray spectroscopy (EDS) (NORAN) in a scanning electron microscope (JEOL, model JSM-6300). Adsorption measurements were performed using a Quantachrome Nova-1000 sorptometer. Specific surface areas were measured by N_2 physisorption at 77 K using BET analysis methods.

The UV–vis absorption spectra of the catalysts were obtained for the dry-pressed disk samples using a Varian Cary 500 UV-Vis spectrophotometer with DRA-CA-30I diffuse reflectance accessory using BaSO_4 as standard reflectance sample.

The crystallinity and structural phase of the catalysts were verified through powder X-ray diffraction (XRD) technique using the $\text{Cu K}\alpha$ source ($\lambda = 1.5406 \text{ \AA}$) of a Bruker D8 Discover diffractometer.

2.3. Soot generation

Soot used in this study was generated by burning pure diesel fuel purchased from Mexican market in a glass vessel with an externally

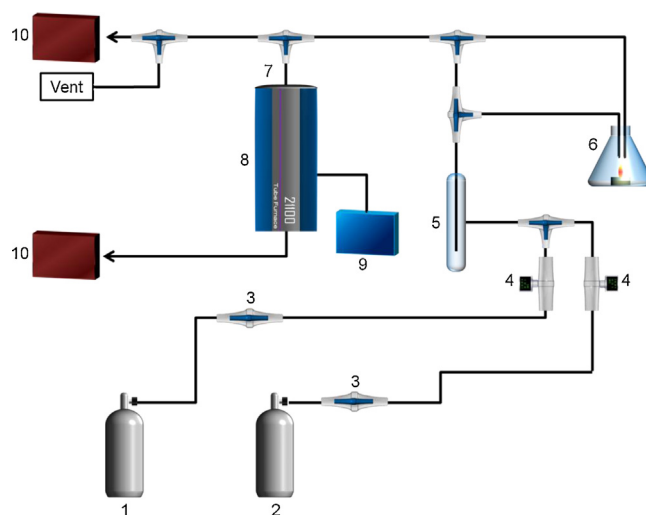


Fig. 1. Schematic diagram of the system used for monitoring the combustion process: (1) N_2 ; (2) O_2 ; (3) switch valve; (4) flow meter; (5) mixer; (6) diesel burner; (7) reactor; (8) furnace; (9) temperature controller; (10) gas chromatograph.

controlled air flow recirculation for 1 h (Fig. 1). The exhaust gas of the vessel was directed to the catalyst sample (200 mg) placed inside a tubular quartz reactor (inner diameter 7 mm) in a programmable furnace. The process was performed using an air feed volume flow rate of $100 \text{ cm}^3 \text{ min}^{-1}$ consisting of 20 vol% of O_2 and 80 vol% of N_2 . The soot generated from the exhaust gas of the vessel, was accumulated on the catalyst in the tubular reactor. After 1 h of diesel combustion, the total amount of soot retained by the catalyst or by the quartz wool was 8.45 mg (measured in a Shimadzu AX200 balance), attaining a soot/catalyst ratio of 0.042.

In order to verify that combustion of the diesel took place in lean conditions, oxygen feed volume flow in the vessel exhaust was monitored by gas chromatography. Oxygen flow remained higher than $10 \text{ cm}^3 \text{ min}^{-1}$ during the combustion process. These results revealed that excess oxygen was present during the diesel combustion.

2.4. Soot oxidation at programmed temperature experiments

After 1 h accumulation of diesel soot over the catalyst surface, air was purged for 15 min to perform soot oxidation. The air (20 vol% of O_2 and 80 vol% of N_2) feeding or flow rate was $100 \text{ cm}^3 \text{ min}^{-1}$. The mixture was heated in the $25\text{--}600^\circ\text{C}$ temperature range with $10^\circ\text{C min}^{-1}$ heating rate, and then cooled down to 25°C . The process comprising soot accumulation on the catalyst at room temperature for 1 h, its subsequent oxidation at increasing temperature and the cooling down process to 25°C is called a cycle. The duration of each cycle was about 2.5 h. Fig. 2 shows the temperature–time profile of a complete cycle. After this first cycle, five similar cycles were performed over the same catalyst sample.

Emission from the reactor was analyzed using a Shimadzu gas chromatograph provided with a thermo-conductivity detector (TCD). The chromatograph used a Porapak column to analyze CO_2 evolutions.

3. Results and discussion

3.1. Catalysts characterization

The catalyst characterization data is summarized in Table 1. It can be seen from the table that during catalyst preparation, the high temperature process in presence of Ag resulted in a strong decrease in specific surface area of calcined SiO_2 . In Table 2 the pore volumes

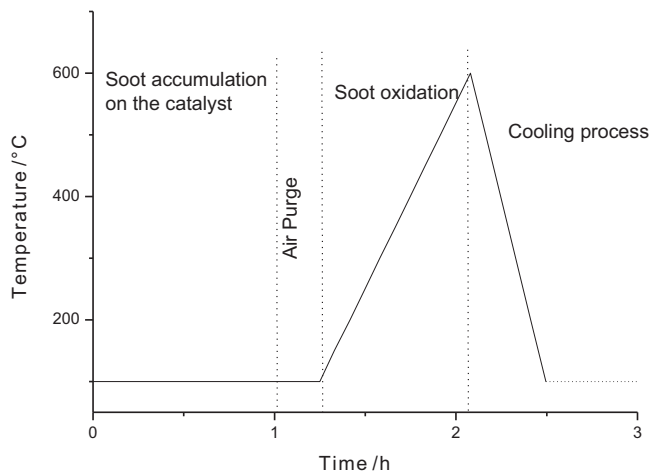


Fig. 2. Temperature–time profile of a complete cycle.

Table 1
Catalysts characterization data.

Catalyst	Silver content (wt%)	Specific surface area ($\text{m}^2 \text{g}^{-1}$)
Calcined SiO_2	–	550
Calcined 3%Ag/ SiO_2	3.1	210
Reduced 3%Ag/ SiO_2	3.1	190

Table 2
Pore size distribution (r_p) and pore volume ($\Delta v/\Delta r_p$) of the fresh catalysts.

Calcined SiO_2		Calcined 3%Ag/ SiO_2		Reduced 3%Ag/ SiO_2	
r_p (nm)	$\Delta v/\Delta r_p$	r_p (nm)	$\Delta v/\Delta r_p$	r_p (nm)	$\Delta v/\Delta r_p$
0.75	5.02	0.75	1.93	0.75	1.74
0.85	10.73	0.85	4.11	0.85	3.72
0.95	11.98	0.95	4.60	0.95	4.16
1.12	21.55	1.12	8.26	1.12	7.48
1.37	21.95	1.37	8.42	1.37	7.62
1.62	22.18	1.62	8.51	1.62	7.70
1.87	18.19	1.87	6.98	1.87	6.31
2.12	15.01	2.12	5.76	2.12	5.21
2.37	12.53	2.37	4.80	2.37	4.35
2.75	9.59	2.75	3.68	2.75	3.33
3.25	6.74	3.25	2.58	3.25	2.34
3.75	4.93	3.75	1.89	3.75	1.71
4.25	3.77	4.25	1.45	4.25	1.31
4.75	2.80	4.75	1.07	4.75	0.97
5.25	2.65	5.25	1.02	5.25	0.92
5.72	2.29	5.72	0.88	5.72	0.79
6.25	1.61	6.25	0.62	6.25	0.56
6.72	1.37	6.72	0.52	6.72	0.47
7.25	1.24	7.25	0.47	7.25	0.43
7.75	1.11	7.75	0.43	7.75	0.39
8.25	0.88	8.25	0.34	8.25	0.30
8.75	0.65	8.75	0.25	8.75	0.23
9.25	0.65	9.25	0.25	9.25	0.23
9.75	0.64	9.75	0.25	9.75	0.22
10.25	0.94	10.25	0.36	10.25	0.33
10.75	0.53	10.75	0.20	10.75	0.18
11.25	0.42	11.25	0.16	11.25	0.15
11.75	0.41	11.75	0.16	11.75	0.14
12.25	0.31	12.25	0.12	12.25	0.11
12.75	0.31	12.75	0.12	12.75	0.11
13.25	0.31	13.25	0.12	13.25	0.11
13.75	0.20	13.75	0.08	13.75	0.07
14.25	0.30	14.25	0.12	14.25	0.11
14.75	0.20	14.75	0.08	14.75	0.07

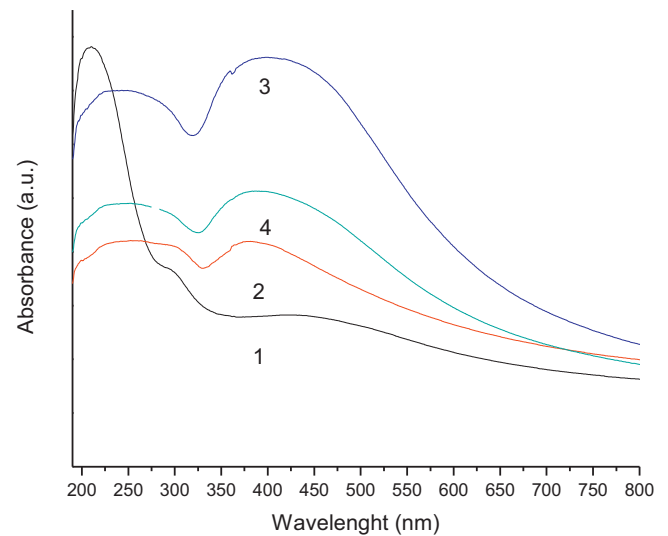


Fig. 3. UV–vis absorption spectra of samples: (1) calcined 3%Ag/ SiO_2 ; (2) calcined 3%Ag/ SiO_2 after 6 oxidation cycles; (3) reduced 3%Ag/ SiO_2 ; (4) reduced 3%Ag/ SiO_2 after 6 oxidation cycles.

and pore size distribution of calcined SiO_2 , calcined 3%Ag/ SiO_2 and reduced 3%Ag/ SiO_2 are reported.

Fig. 3 presents the UV–vis absorption spectra for the calcined 3%Ag/ SiO_2 and reduced 3%Ag/ SiO_2 before and after performing 6 soot oxidation cycles.

The main features that can be identified from the reduced 3%Ag/ SiO_2 absorption spectra are: A broad signal spreading through 320 and 600 nm, which can be ascribed to the overlapping of silver SPR signal (400–550 nm) with the σ – σ^* and n – σ^* transition signals of Ag_n clusters appear in the 330–360 nm and 440–540 nm spectral range, respectively [40,41]. It can be seen that there are no appreciable differences between the absorption spectra of the reduced 3%Ag/ SiO_2 sample before (spectrum 3) and after diesel soot oxidation cycles (spectrum 4). The result suggests that the electronic state of silver in reduced 3%Ag/ SiO_2 remained the same even after six diesel soot oxidation cycles.

The small hump appeared at about 310 nm for the calcined 3%Ag/ SiO_2 sample (spectrum 1) is associated with the absorption of Ag^0 (250–320 nm). For this catalyst, presence of an intense absorption band in the 190 and 230 nm spectral range (peaked at about 215 nm), indicates the presence of Ag^+ ions on the surface of the catalyst [42]. The band disappeared almost completely after the diesel soot oxidation cycles (spectrum 2). However, the signals in between 250 and 320 nm, characteristic of Ag^0 , the signals characteristic of Ag_n clusters (330–360 nm), and of silver SPR (400–550 nm) increased after performing the diesel soot oxidation cycles, suggesting a reduction of Ag^+ ions present in the calcined 3%Ag/ SiO_2 to Ag^0 during diesel soot oxidation process.

In Fig. 4, the XRD patterns of the calcined 3%Ag/ SiO_2 sample before and after its use in soot oxidation process (6 cycles) are presented. The calcined 3%Ag/ SiO_2 sample revealed only two weak diffraction peaks correspond to the (2 0 0) and (1 1 0) lattice planes of cubic Ag_2O_3 (JCPDS # 72-0607) and hexagonal Ag_2O (JCPDS # 72-2108), respectively. There appeared no diffraction peak associated to metallic Ag in this sample. After its use in soot oxidation process, the sample revealed four clear diffraction peaks of metallic Ag (JCPDS # 87-0717) of hexagonal phase, along with a weak peak associated to cubic Ag_2O . Evolution of XRD peaks of metallic silver in the sample after its use in soot oxidation process clearly indicates the reduction of silver ions during the catalytic process, as has also been observed in its optical absorption study.

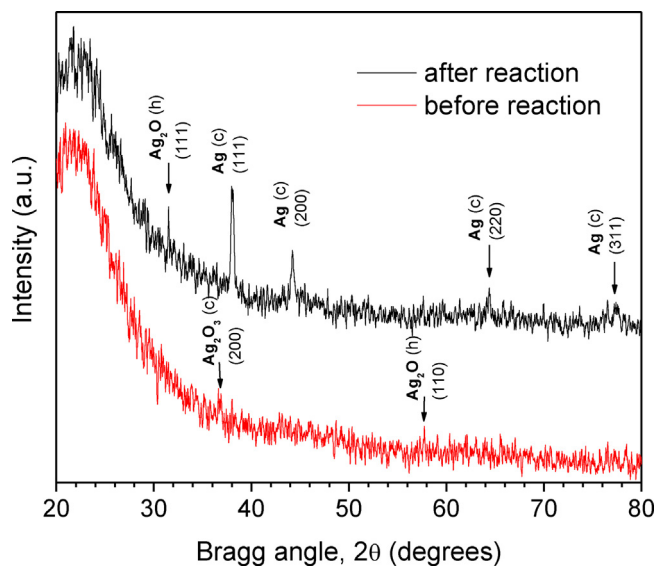


Fig. 4. XRD patterns of the calcined 3%Ag/SiO₂ catalyst before and after 6 cycles of soot oxidation process.

3.2. Soot oxidation on quartz wool

Fig. 5 shows the effect of temperature on soot oxidation over quartz wool. As can be seen, CO₂ evolution as a function of temperature revealed two well resolved peaks. The first peak appeared at about 450 °C and the second peak at higher temperature (>700 °C).

From Fig. 5, we can observe that in the absence of an oxidation catalyst, very low amounts of CO₂ could be detected during the soot oxidation reaction at temperatures between 25 and 600 °C. The total area under the CO₂ evolution curve in between 25 and 800 °C [CO₂]_{Ref} determined over quartz wool is taken as a measure of the total amount of carbon in the soot generated from the exhaust gas of the vessel and accumulated for 1 h. The catalytic efficiency of the catalyst was calculated from the estimated [CO₂] evolved during the catalytic process and the same while using only quartz wool as:

$$\text{Catalyst efficiency} = \frac{[\text{CO}_2]_{\text{Cat}}}{[\text{CO}_2]_{\text{Ref}}}$$

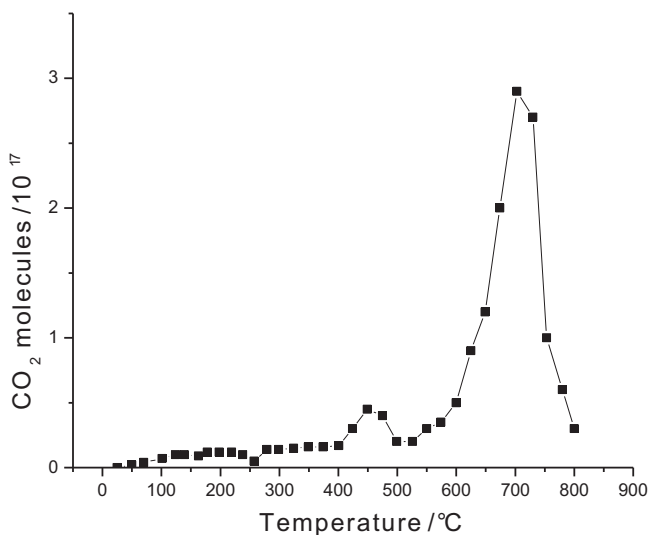


Fig. 5. Effect of temperature on the diesel soot oxidation over quartz wool. Feed: 20 vol% of O₂, and 80 vol% of N₂.

Table 3

Total areas and T_{max} values from diesel soot oxidation experiments (from 25 to 600 °C) for the 1st, 2nd, and 6th oxidation cycles on the catalysts.

Catalyst	Area (CO ₂ molecules E+18 °C)			T_{max} (°C)		
	1st	2nd	6th	1st	2nd	6th
Calcined SiO ₂	9.2	11.1	9.4	362	365	379
Calcined 3%Ag/SiO ₂	228	339	305	330	222	250
Reduced 3%Ag/SiO ₂	321	349	365	237	205	216
Calcined SiO ₂ + calcined 3%Ag/SiO ₂	408	361	429	250	240	251

Table 4

Catalyst efficiency values of the catalysts during the 1st, 2nd, and 6th oxidation cycles.

Catalyst	Catalyst efficiency		
	1st	2nd	6th
Calcined SiO ₂	0.02	0.02	0.02
Calcined 3%Ag/SiO ₂	0.50	0.75	0.65
Reduced 3%Ag/SiO ₂	0.71	0.77	0.80
Calcined SiO ₂ + calcined 3%Ag/SiO ₂	0.90	0.80	0.95

where [CO₂]_{Cat} is the area under CO₂ curve (soot oxidation evolution in between 25 and 600 °C) measured over the catalyst, and [CO₂]_{Ref} is the area under CO₂ curve (soot oxidation evolution from 25 to 800 °C) measured over the quartz wool (=451 × 10¹⁸ CO₂ molecules °C). The [CO₂]_{Cat} and calculated catalytic efficiency values of both the calcined and reduced catalysts are presented in Tables 3 and 4.

3.3. Soot oxidation over calcined SiO₂

The results of soot oxidation experiments over calcined SiO₂ are presented in Fig. 6. As can be seen, for all the oxidation cycles, CO₂ evolution curves revealed a small signal at about 350 °C, and the intensity of this signal did not vary appreciably from cycle to cycle. In order to investigate if this low amount of detected CO₂ was due to the poor oxidation activity of calcined SiO₂ or due to a low amount of retained soot, the first soot oxidation cycle was performed from 25 to 800 °C. As can be seen in Fig. 6, the CO₂ evolution curve corresponding to this first diesel soot oxidation cycle presents a similar behavior as that of the diesel soot oxidation over quartz wool (Fig. 5). However, the first signal detected at about

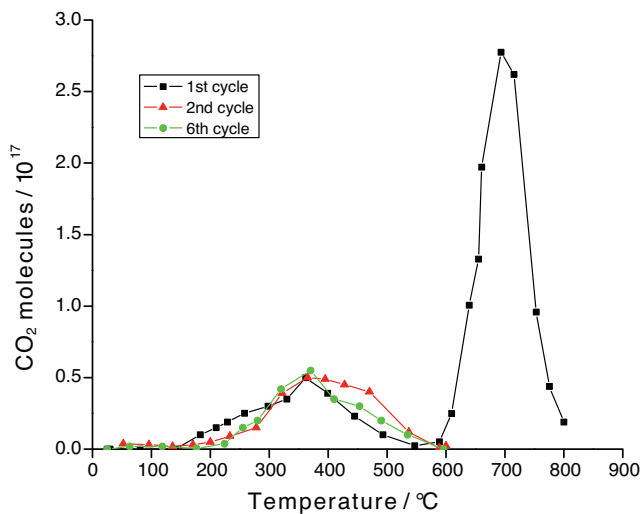


Fig. 6. Evolution of CO₂ molecules/g cat. as a function of the soot oxidation temperature over calcined SiO₂.

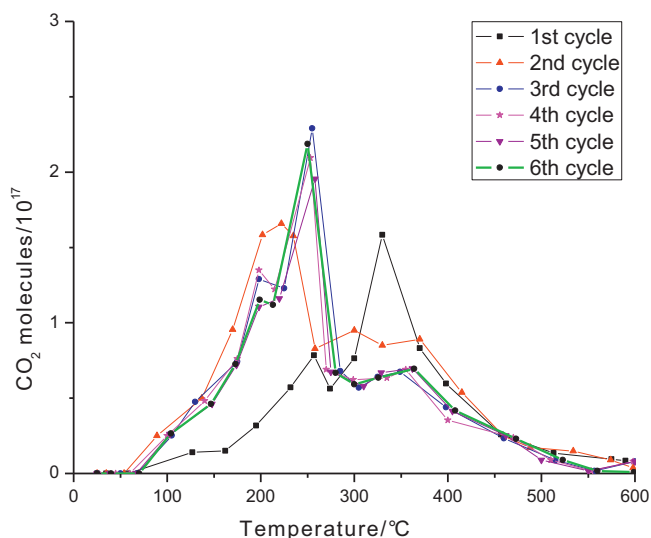


Fig. 7. Evolution of CO₂ molecules/g cat. as a function of the soot oxidation temperature, over the calcined 3%Ag/SiO₂ catalyst.

450 °C for quartz wool was detected at about 350 °C for the calcined SiO₂. This shift of signal to lower temperature is probably due to the catalytic effect of the calcined SiO₂. The second peak which appeared at high temperatures (>700 °C) during diesel soot oxidation over quartz wool is similar to that obtained over the calcined SiO₂. These results suggest the following facts:

- Similar amounts of diesel soot are retained over the quartz wool and the calcined SiO₂.
- Effectively, the calcined SiO₂ catalyzes only a small fraction of the deposited diesel soot.

3.4. Soot oxidation over calcined 3%Ag/SiO₂

The effect of temperature on soot oxidation over calcined 3%Ag/SiO₂ is shown in Fig. 7. The CO₂ evolution curve as a function of temperature revealed that:

- During the first oxidation cycle, the temperature of maximum soot oxidation (T_{max}) is 350 °C.
- During the subsequent cycles, the T_{max} value markedly decreases from 350 to 230 °C.

The above results indicate that during the first oxidation cycle, a change of the electronic state of Ag might have taken place. It has been reported that the enthalpy of formation of bulk Ag₂O ($-\Delta H_f$) is very low (7 kcal/mol) [43]. When a metal oxide with low ($-\Delta H_f$) is once converted to metallic species, its reoxidation is more difficult than the metal oxides with high ($-\Delta H_f$). Thus, the metal oxides with low ($-\Delta H_f$) value cannot act as catalysts for soot oxidation when the oxide is once thermally decomposed or reduced by carbon during soot oxidation. However, in Fig. 7, it can be seen that during the second and sixth soot oxidation cycles over the calcined catalyst, the T_{max} value markedly decreased (from 350 to 230 °C) with an increase in the surface area. Table 4 shows that the catalytic efficiency calculated for this catalyst increases during the 2nd to the 6th cycle. These results can be explained assuming that:

- During the first cycle, Ag₂O present in calcined 3%Ag/SiO₂ acted as a strong stoichiometric oxidant for soot combustion and is reduced by carbon to metallic Ag⁰.

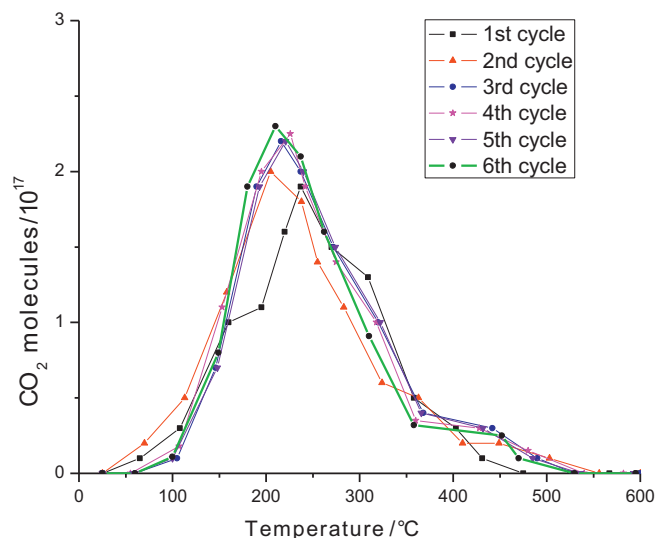


Fig. 8. Evolution of CO₂ molecules/g cat. as a function of the soot oxidation temperature over reduced 3%Ag/SiO₂ catalyst.

During the subsequent cycles, Ag acts as a metallic catalyst promoting the formation of superoxide ions (O₂⁻), as has been demonstrated earlier [43–47]. It is well known that metallic silver is an oxidation catalyst that can form several suboxide species (oxygen adatom, superoxide ion, subsurface oxygen, oxygen adatoms, and oxydic oxygen adatoms) in oxidation atmosphere [14,15,19,48–50]. Nakatsuji et al. have studied the mechanism of silver-catalyzed partial oxidation by theoretical calculations using the ab initio second order Møller–Plesset (MP2) method combined with the dipped adcluster model (DAM) [51,52]. They concluded that the active species was superoxide ion O₂⁻, which was molecularly adsorbed in bent end-on geometry on the silver surface. Moreover, Anegi et al. [22] have pointed out recently that the superoxide ions generated by metallic silver might assist carbon oxidation.

- These assumptions are supported by the results obtained both from the UV–vis absorption spectra and XRD spectra of the calcined 3%Ag/SiO₂ catalyst before and after 6 diesel soot oxidation cycles, which confirm the reduction of Ag⁺ to Ag⁰ during the soot oxidation cycles.

3.5. Soot oxidation over reduced 3%Ag/SiO₂

Fig. 8 shows the evolution of CO₂ as a function of the diesel soot oxidation temperature over the reduced 3%Ag/SiO₂. From the figure, we can see that during the six soot oxidation cycles, the T_{max} remained unaltered (~250 °C). Moreover, the surface area and the catalytic efficiency values calculated for the three curves are very similar as shown in Tables 3 and 4. Similar results obtained for the three diesel soot oxidation cycles over the reduced 3%Ag/SiO₂ suggest that during soot oxidation process, the electronic state of Ag did not change. Thus the active silver present over the surface of the fresh catalyst (not used for soot oxidation) remained in its metallic state during the soot oxidation cycles. The results obtained from the UV–vis absorption spectra of the reduced 3%Ag/SiO₂ catalyst before and after 6 diesel soot oxidation cycles (Fig. 3) support this assumption. The above results indicate that this catalyst is thermally stable and can operate at the temperatures of diesel engine exhaust gases.

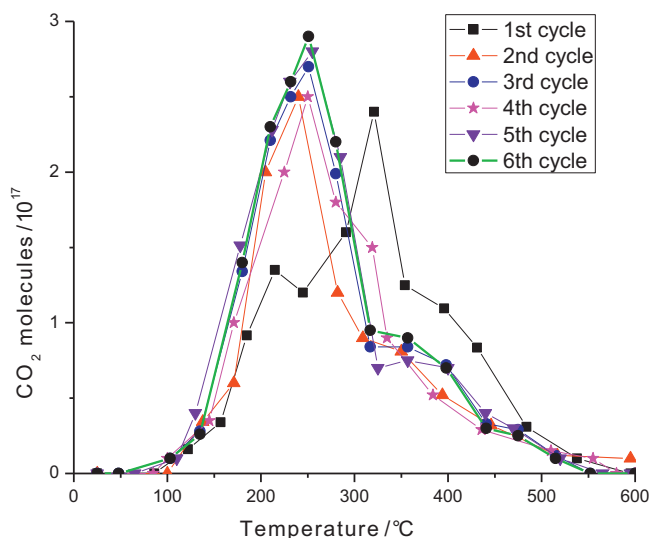


Fig. 9. Evolution of CO₂ molecules/g cat. as a function of the soot oxidation temperature over the mixture calcined 3%Ag/SiO₂ + calcined SiO₂.

3.6. Soot oxidation over calcined 3%Ag/SiO₂ + SiO₂

In order to determine the effect of high specific surface area of fumed SiO₂ on the soot particle interactions, the diesel soot oxidation process was investigated over a mechanical mixture of 0.2 g of calcined 3%Ag/SiO₂ and 0.2 g of calcined SiO₂. Six soot oxidation cycles were performed over the mixture. Results presented in Fig. 9 show that the temperature evolution of CO₂ over the catalyst mixture presents similar T_{max} as that of the calcined 3%Ag/SiO₂ alone. However, the areas under the CO₂ evolution curves determined for the six cycles in the 25–600 °C temperature range and the calculated catalytic efficiency values were higher over the catalyst mixture than that of the calcined 3%Ag/SiO₂ alone (Tables 3 and 4).

The enhanced catalytic activity of the mixture can be understood considering that during diesel burning, produced soot was accumulated in the pores of the catalyst. Table 2 shows the pore size distribution of the catalysts ranging in between 0.7 and 15 nm. It is worth noting that the calcined SiO₂ presents a higher pore volume than the Ag/SiO₂ catalysts, which may result in a stronger soot accumulation. On the other hand, Braun et al. [53], distinguished, by TEM and SAXS analysis obtained from diesel soots, a soot particle aggregate size ranging between 70 and 100 nm; a primary particulate size that was typically 10–20 nm, and the particulate subunit size which was ~2 nm. The diesel soot particles ranging from 2 to 15 nm may be deposited in the suitable sized pores of the 3%Ag/SiO₂–SiO₂ mixture.

As the diffusion rate of the produced gases during soot oxidation process reduces while passing through the pores in calcined SiO₂, the probability of interaction of the soot particles with the O₂[−] produced by metallic Ag increases greatly, resulting in an increase of oxidation rate of the soot particles. This increased interaction between O₂[−] and soot particles in the calcined SiO₂ pores indicates that the use of a 3%Ag/SiO₂ + SiO₂ mixture might be a more suitable substitute of fuel borne catalyst additives or molten salts catalysts for diesel soot oxidation.

4. Conclusions

Catalyzed diesel soot filters are regarded as the most promising solution to reduce the emission of particulate matter from diesel engines. However, low catalytic activity and poor soot–catalyst contact at lower temperatures are still the problems for their practical applications. We have developed a 3%Ag/SiO₂ catalyst which is

an effective catalyst for diesel soot oxidation at low temperatures (150–300 °C), presenting high soot–catalyst contact. The catalyst is highly stable during several consecutive reaction cycles. The results obtained over the calcined and reduced samples indicate that metallic silver is the active species during the oxidation reaction. Metallic silver can promote the formation of superoxide ions (O₂[−]) which play a key role in the diesel soot oxidation process. Increased soot oxidation rate over the mechanical mixture of 3%Ag/SiO₂ and SiO₂ is due to the increased interactions of O₂[−] with primary soot particles and subunits deposited into the porous structure of the 3%Ag/SiO₂–SiO₂ mixture.

Acknowledgments

The authors are pleased to acknowledge valuable support for this research from CONACYT (Grant # 130389), from the Puebla (Mexico) State Government, and from Vicerrectoria de Investigación y Estudios de Posgrado (BUAP), Grant # 36/NAT/12.

References

- [1] M. Shelef, R.W. McCabe, Catalysis Today 62 (2000) 35.
- [2] P. Selenka, W. Cartelleri, P. Herzog, Applied Catalysis B 10 (1996) 3.
- [3] M. Schejbal, J. Stepanek, M. Marek, P. Koci, M. Kubicek, Fuel 89 (2010) 2365.
- [4] B.A.A.L. van Setten, M. Makkee, J.A. Moulijn, Catalysis Reviews: Science and Engineering 43 (2001) 489.
- [5] B.A.A.L. van Setten, J.M. Schouten, M. Makkee, J.A. Moulijn, Applied Catalysis B 28 (2000) 253.
- [6] P. Ciambelli, V. Palma, P. Russo, S. Vaccaro, Journal of Molecular Catalysis A 204–205 (2003) 673.
- [7] G. Saracco, C. Badini, N. Russo, V. Specchia, Applied Catalysis B 21 (1999) 233.
- [8] M. Jequirim, V. Tshamber, J.F. Brilac, P. Ehrburger, Fuel 84 (2005) 1949.
- [9] M.L. Pisasrello, V. Milt, M.A. Peralta, C.A. Querini, Catalysis Today 75 (2002) 465.
- [10] V.G. Milt, C.A. Querini, E.E. Miro, M.A. Ulla, Journal of Catalysis 220 (2003) 424.
- [11] Y. Shirashi, N. Toshima, Journal of Molecular Catalysis A 141 (1999) 187.
- [12] J.P.A. Neeft, M. Makkee, J.A. Moulijn, Fuel 77 (1998) 111.
- [13] A.N. Pestrakov, Catalysis Today 28 (1996) 239.
- [14] Lj. Kundakovic, M. Flytzani-Stephanopolus, Applied Catalysis A 183 (1999) 35.
- [15] A. Nagy, G. Mestl, Applied Catalysis A 188 (1999) 337.
- [16] P.W. Park, C.L. Boyer, Applied Catalysis B 59 (2005) 27.
- [17] R. Brosius, K. Arve, M.H. Groothaert, J.A. Martens, Journal of Catalysis 231 (2005) 344.
- [18] S. Immamura, H. Yamada, K. Utani, Applied Catalysis A 192 (2000) 221.
- [19] Z. Qu, M. Cheng, W. Huang, X. Bao, Journal of Catalysis 229 (2005) 446.
- [20] M. Luo, X. Yuan, X. Zheng, Applied Catalysis A 175 (1998) 121.
- [21] L.L. Murrel, R.T. Carlin, Journal of Catalysis 159 (1996) 479.
- [22] E. Aneggi, J. Llorca, C. Leitenburg, G. Dolcetti, A. Trovarelli, Applied Catalysis B 91 (2009) 489.
- [23] K. Villani, R. Brosius, J.A. Martens, Journal of Catalysis 236 (2005) 172.
- [24] R. Burch, J.P. Breen, F.C. Meunier, Applied Catalysis B 39 (2002) 283.
- [25] B.M. Weckhuysen, R.A. Schoonheydt, Catalysis Today 49 (1999) 441.
- [26] J. Melsheimer, M. Thiede, R. Ahmad, G. Tzolova-Müller, F.C. Jentoft, Physical Chemistry Chemical Physics 5 (2003) 4366.
- [27] X. Gao, J.-M. Jehng, I.E. Wachs, Journal of Catalysis 209 (2002) 43.
- [28] M.D. Argyle, K. Chen, C. Resini, C. Krebs, A.T. Bell, E. Iglesia, Journal of Physical Chemistry B 109 (2004) 2345.
- [29] R. Ahmad, J. Melsheimer, F.C. Jentoft, R. Schlögl, Journal of Catalysis 218 (2003) 365.
- [30] U. Kreibig, M. Vollmer, Optical Properties of Metal Clusters, Springer, Berlin, 1995.
- [31] A.N. Pestrakov, A.A. Davydov, Journal of Electron Spectroscopy and Related Phenomena 74 (1995) 195.
- [32] K.L. Kelly, E. Coronado, L.L. Zhao, G.C. Schatz, Journal of Physical Chemistry B 107 (2003) 668.
- [33] C. Sönnichsen, T. Franzl, T. Wilk, G. von Plessen, J. Feldmann, New Journal of Physics 93 (2002) 1.
- [34] F. Stietz, F. Träger, Philosophical Magazine B 79 (1999) 1281.
- [35] J.J. Mock, M. Barbic, D.R. Smith, D.A. Schultz, S. Schultz, Journal of Chemical Physics 116 (2002) 6755.
- [36] P. Mulvaney, Langmuir 12 (1996) 788.
- [37] A. Hilger, M. Tenfelde, U. Kreibig, Applied Physics B 73 (2001) 361.
- [38] T. Jensen, L. Kelly, A. Lazarides, G.C. Schatz, Journal of Cluster Science 10 (1999) 295.
- [39] U. Kreibig, L. Genzel, Surface Science 156 (1985) 678.
- [40] G.A. Ozin, H. Huber, Inorganic Chemistry 17 (1978) 155.
- [41] S.A. Mitchell, G.A. Kenney-Wallace, G.A. Ozin, Journal of the American Chemical Society 103 (1983) 6030.
- [42] J. Texier, J.J. Hastrelter, J.L. Hall, Journal of Physical Chemistry 87 (1983) 4690.
- [43] D.E. Fein, I.E. Wachs, Journal of Catalysis 210 (2002) 241.
- [44] R.B. Clarkson, Journal of Catalysis 33 (1974) 392.

- [45] A. Aboukais, M. Jarjoui, J.C. Verdrine, P.C. Gravelle, *Journal of Catalysis* 47 (1977) 399.
- [46] S. Tanaka, T. Yamashina, *Journal of Catalysis* 40 (1975) 140.
- [47] M. Machida, Y. Murata, K. Kishikawa, D. Zhang, K. Ikeue, *Chemistry of Materials* 20 (2008) 4489–4494.
- [48] N. Gungor, S. Gunister, W. Mista, H. Teterycz, R. Klimkiewicz, *Applied Clay Science* 32 (2006) 291.
- [49] Z. Qu, M. Chen, X. Dong, X. Bao, *Catalysis Today* 93–95 (2004) 247.
- [50] G.I.N. Waterhouse, G.A. Bowmaker, J.B. Metson, *Applied Surface Science* 214 (2003) 36.
- [51] H. Nakatsuji, Z.M. Hu, H. Nakai, *International Journal of Quantum Chemistry* 65 (1997) 839–855.
- [52] H. Nakatsuji, *International Journal of Quantum Chemistry* 42 (1992) 725.
- [53] A. Braun, F.E. Huggins, S. Seifert, J. Ilavsky, N. Shah, K.E. Kelly, A. Sarofim, G.P. Huffman, *Combustion and Flame* 137 (2004) 63.